Accelerated loss of hypoxia response and biased allele expression in zebrafish with Alzheimer's disease-like mutations

Morgan Newman[1*], Hani Moussavi Nik[1], Greg T. Sutherland[2] , Woojin S. Kim[3,4], Glenda M. Halliday[3,4], Suman Jayadev[5], Carole Smith[5], Thaksaon Kittipassorn[1,6], Dan J. Peet[1], and Michael Lardelli[1]

[1]School of Biological Sciences, University of Adelaide, Adelaide, SA, Australia.

[2]Discipline of Pathology, School of Medical Sciences and Charles Perkins Centre, Faculty of Medicine and Health, The University of Sydney, Camperdown, NSW, Australia.

[3] Brain and Mind Centre, Central Clinical School, Faculty of Medicine and Health, The University of Sydney, Camperdown, NSW, Australia.

[4] School of Medical Sciences, University of New South Wales & Neuroscience Research Australia, Randwick NSW, Australia

[5] Department of Neurology, University of Washington, Seattle, Washington, USA.

[6] Department of Physiology, Faculty of Medicine Siriraj Hospital, Mahidol University, Bangkok, Thailand

*Corresponding author: morgan.newman@adelaide.edu.au

Abstract

Ageing is the major risk factor for Alzheimer's disease (AD), a condition involving brain hypoxia. Expression of transcriptional regulator of cellular responses to hypoxia, HYPOXIA-INDUCIBLE FACTOR-1 (HIF1), increases with brain age. HIF1 interacts with PRESENILIN 1 (PSEN1), the major locus for mutations causing familial AD (fAD). We introduced two fAD-like mutations into zebrafish *psen1* and analysed their effects on HIF1-controlled gene expression in brains. Mutant *psen1* alleles accelerated age-dependent changes in HIF1-controlled gene expression. Also, aged brains shifted into an unexpected state where HIF1-controlled genes show "inverted" responses to hypoxia. Intriguingly, zebrafish *psen1* expression was biased towards mutant *psen1* alleles over wild type alleles in an age- and hypoxia-dependent manner. Brains of human *PSEN1* fAD mutation carriers showed reduced *PSEN1* mRNA expression but no allelic bias. Our results are consistent with "molecular ageing" being a necessary precondition for AD and with AD identifiable as a distinct, pathological brain molecular state.

Introduction

Alzheimer's disease (AD) is the most prevalent form of dementia. Decreased levels of soluble amyloid-beta (Aβ) peptides in cerebrospinal fluid [1] (presumably due to decreased clearance from the brain) is regarded as one of the earliest markers of both early-onset familial AD (fAD) and late-onset sporadic AD (LOAD), preceding disease onset by 20-30 years [2, 3], while vascular changes may occur even earlier [4]. When AD clinical symptoms finally become overt, neurodegeneration may be too advanced for effective therapeutic intervention. This may explain the failure of drugs designed to inhibit supposed Aβ-related pathological processes to halt cognitive decline [5, 6].

The molecular events underlying LOAD are complex and have eluded detailed understanding. However, fAD is caused by inherited, dominant mutations in the genes, *PRESENILIN 1* (*PSEN1*), *PRESENILIN2* (*PSEN2*), *AMYLOID BETA A4 PRECURSOR PROTEIN* (*APP*) and *SORTILIN-RELATED RECEPTOR* (*SORL1*) [7],[8] and so is amenable to genetic analysis in animal models. Less than two percent of AD is defined as fAD. However, the similarity in clinical disease progression and brain pathology of fAD and LOAD [9] has led researchers to assume that genetic analysis of fAD will contribute to understanding of both forms of the disease. Given that PSEN1 and PSEN2 are alternative components of the γ-secretase complex most fAD research is focussed on APP as the source of the Aβ peptide. *PSEN* mutations are viewed mostly as altering cleavage of APP to yield changes in the relative abundance of different Aβ size forms. However, on a population basis, the majority of fAD

mutations occur in the gene *PSEN1* [10] and the relationship between fAD mutations in the *PRESENILIN* genes and *APP* is still a matter of debate [11, 12].

Analysis of various structural and functional brain images (MRI and/or PET) from individuals with fAD mutations has revealed changes as early as nine years of age [13, 14]. Specifically, elevations in Aβ deposition and reduced glucose metabolism have been observed in the brain years before symptom onset [15]. Surprisingly, there has been little detailed molecular investigation of the young adult brains of any animal model closely mimicking the human fAD genetic state – i.e. heterozygous for a fAD-like mutation in a single, endogenous gene. Consequently, to model and explore early changes in the brain driving AD pathogenesis, we have edited the zebrafish genome to introduce fAD-like mutations into the endogenous, *PSEN1*-equivalent gene of zebrafish, *psen1*. Our recent transcriptomic analysis of one such mutation, *psen1*^{K97fs}, revealed acceleration of elements of brain aging (*Hin et al., 2018 submitted*).

Cardiovascular risk factors strongly correlate with LOAD [16, 17]. Other significant risk factors include vascular brain injury and traumatic brain injury [18], while recent studies suggest that aerobic exercise can reduce AD risk [19, 20]. Reduced blood flow has been observed in AD brains (reviewed by [21, 22]) which would lead to impaired oxygenation, resulting in hypoxia. Hypoxia is able to induce the expression of the fAD genes [23, 24] and a serum biomarker associated with hypoxia can discriminate between people with Mild Cognitive Impairment (MCI) who progress to AD and those who do not [25] supporting a critical involvement of hypoxia in AD pathogenesis. These connections between AD and hypoxia led us to test the responses

to acute hypoxia of our fAD mutation-like zebrafish models at various ages. Zebrafish are a versatile model organism for genetic analyses of acute hypoxic responses. We found that genetic responses to hypoxia and, particularly, allele-specific expression, increase greatly with age but that extremely aged fish brains "invert" to show the opposite responses. Two very different fAD-like mutations in *psen1* both accelerate the onset of this inversion. In addition, the expression of mutant and wild type allele transcripts is biased towards the mutants, with a dramatic loss of wild-type *psen1* expression which becomes more extreme with age and acute hypoxia. This loss of *PSEN1* expression is also observed in human fAD brain tissue and would contribute to loss of normal gene function in the disease.

Results

Age favours expression of the mutant psen1 alleles

The zebrafish *psen1*^{K97fs} (hereafter "K97fs") mutation is similar to the unique, human frame-shifting fAD mutation *PSEN2*^{K115fs} [8]. This mutation mimics a hypoxia-induced truncated isoform of PSEN2 protein, PS2V, that is upregulated in LOAD brains [26-28]. During editing of this mutation into the zebrafish genome (*Hin et al., submitted*) we isolated a second mutation at the same site, *psen1*$^{Q96\_K97del}$ (hereafter "Q96_K97del"). This is a deletion of two codons that maintains the open reading frame and is predicted to alter the structure of the first luminal loop of the zebrafish Psen1 protein, similar to numerous fAD mutations in human *PSEN1* [11, 29].

To establish that the fAD-like mutant alleles of zebrafish *psen1* are expressed, we performed digital, quantitative PCR (dqPCR) on cDNA synthesised from total RNA extracted from zebrafish brain at 6 months (young adults) and 24 months (old adults).

In young adults, *K97fs* transcripts are present at approximately half the level of wild type transcripts (Figure 1A) and so have escaped complete nonsense mediated decay (NMD), despite their possession of a premature stop codon. In contrast, *Q96_K97del* transcripts are present at levels approximately 1.7-fold higher than the wild type transcript (Figure 1B). By 24 months of age, the expression level of the *K97fs* transcripts in mutant brains has inverted to more than double the level of the wild type transcripts. For the *Q96_K97del* mutation the excess of mutant over wild type transcript has increased to 4.2-fold. The observed increase in the mutant transcript is accompanied by a dramatic decrease in wild type transcript expression in the aged mutant brains. The wild type transcript in the 24 month old wild type fish brains is present at levels ~6.5-fold higher than in *Q96_K97del/+* sibling brains and ~4-fold higher than in *K97fs/+* sibling brains. This loss of wild type *psen1* transcript and increase in mutant transcript presumably has significant effects on normal *psen1* function in the aged mutant fish.

Hypoxia further biases psen1 allele expression

Acute hypoxia increases expression of fAD genes, including the *PRESENILIN*s [23, 24], and hypoxia has also been associated with AD risk and pathogenesis [30]. Therefore, we tested the effect of acute hypoxia on the bias in allele expression in young and aged adult zebrafish brains. Gene expression responses to hypoxia can be induced by exposure of zebrafish to oxygen-depleted water for ~2.5 hours (oxygen concentration of 6.6 ± 0.5 mg/L in normoxia and 1.1 ± 0.5mg/L in hypoxia [23, 31]). For both the *K97fs* and *Q96_K97del* alleles, hypoxia increased allelic expression bias (Figure 1A and B). In both young and old mutant zebrafish brains, acute hypoxia greatly favours expression of the mutant transcripts over the wild type transcripts. In

young adult mutant zebrafish, hypoxia inverted the relative ratio of *K97fs* and wild type allele expression seen under normoxia so that it resembled the biased expression observed in the aged mutant brains. In the aged mutant brains, hypoxia increased the excessive transcript expression of the *K97fs* allele over the wild type allele to 6.4-fold (Figure 1A). Similarly, the excess of *Q96_K97del* mutant transcript over wild type transcript in young adult mutant zebrafish brains under hypoxia is similar to the ratio of allele expression in aged mutant brains under normoxia. Hypoxia in the aged mutant brains increases the excess of mutant over wild type allele expression to 10.8-fold (Figure 1B). The similar ratios of mutant over wild type allele expression in young hypoxic and aged "normoxic" mutant brains are consistent with hypoxic stress being a normal aspect of brain aging.

Accelerated loss of HIF-1-responses in aging mutant zebrafish brains

The bipartite transcription factor, hypoxia-inducible factor 1 (HIF-1), controls many of the cellular responses to hypoxia. Under hypoxia, HIF-1 binds to hypoxia response elements in promoter sequences to induce the transcription of numerous HIF-1-responsive genes (HRGs, reviewed by [32]). These include the gene *PDK1* encoding PYRUVATE DEHYDROGENASE KINASE1 that phosphorylates PYRUVATE DEHYDROGENASE to inhibit conversion of pyruvate to acetyl-CoA [33]. In this way, pyruvate is directed away from the tricarboxylic acid cycle (TCA) and oxidative phosphorylation and into ATP production via anaerobic glycolysis. Thus, PDK1 acts as a form of "rheostat" to set the relative rates of anaerobic glycolysis and oxidative phosphorylation. To determine the effects of age and the fAD-like alleles of *psen1* on HIF1-directed responses to hypoxia, we used dqPCR to compare transcript levels

from five HRGs: *cd44a*, *edn1*, *igfbp3*, *mmp2* (reviewed in [34]) and *pdk1* [35] in the brains of zebrafish exposed to normoxia or acute hypoxia.

Unexpectedly, the responses of heterozygous zebrafish carrying either fAD-like allele were essentially identical and very different from those of wild type siblings (Figure 2A, B). Young, 6-month-old mutants show raised basal levels of HRG expression under normoxia suggestive of pre-existing hypoxic stress, although other explanations are possible such as alteration of iron homeostasis or alteration of basal γ-secretase levels (see the Discussion). Nevertheless, both wild type and mutant young adult zebrafish were able to increase HRG expression under acute hypoxia. Aged, 24-month-old zebrafish showed increased basal HRG expression under normoxia, similar to the young mutants. This is consistent with our previous observations that a fAD-like mutation of *psen1* accelerates brain aging (*Hin et al., 2018 submitted*). Despite this raised basal level of HRG expression, 24-month-old wild type brains approximately double their level of HRG expression under hypoxia. Interestingly, their levels of HRG expression are then essentially identical to those in 24-month-old fAD-like zebrafish brains under normoxia, once again supporting that the aged fAD brains are under hypoxic stress.

The greatest surprise came when the 24-month-old, aged brains heterozygous for either mutant allele of *psen1*were subjected to acute hypoxia. Rather than upregulating HRG expression, they either failed to upregulate, or even downregulated, HRG expression. This inversion of the expected hypoxia response was particularly noticeable for expression of *pdk1*, suggesting an inability to upregulate anaerobic glycolysis in aged fAD-like mutant zebrafish under hypoxia.

Assays of lactate content (a marker of anaerobic glycolysis) in young and aged adults also revealed a failure to upregulate anaerobic glycolysis in the aged *Q96_K97del* heterozygous mutants under acute hypoxia, which is largely consistent with our observations of age-dependent *pdk1* expression behaviour (Figure 3). However, in contrast to *pdk1* expression, there is no apparent upregulation of anaerobic glycolysis in young wild type brains under acute hypoxia (an observation also reported in young mouse brains under chronic hypoxia [36]).

Wild type fish also lose HIF-1-responses with age

Our previous transcriptome analysis of heterozygous *K97fs* mutant zebrafish brains demonstrated accelerated aging in these fAD-like mutants and an "inverted" pattern of differential gene expression once these became aged (24 months). We now see that this gene expression inversion is associated with failure of hypoxia responses including failure to upregulate glycolysis under hypoxia. If fAD-like mutations accelerate brain aging, do wild type brains eventually show the same failure of HRG expression as they age? To test this we examined *Q96_K97del* heterozygous and wild type sibling brains under normoxia or acute hypoxia at 42 months of age (Figure 2B). (Laboratory-reared zebrafish are reported to have a mean life span of ~42 months [37], and we were fortunate enough to have *Q96_K97del* heterozygous and wild type siblings surviving to this extreme age). The levels of HRG expression in brains of both genotypes are essentially the same under normoxia, and both genotypes show downregulation of HRG expression under acute hypoxia. This clearly supports that

fAD-like mutations accelerate brain aging and that a failure to upregulate HRG expression under acute hypoxia may be an inevitable consequence of aging.

The psen1 fAD-like alleles variably affect Hif-1α stability

The bipartite transcription factor HIF-1 is formed by complexation of subunits HIF-1α and HIF-1β. The stability of HIF-1α (and, hence, the level of HIF-1) is controlled by oxygen availability (reviewed by [32]). Stabilisation of HIF-1α under hypoxia has been shown to depend, partially, on interaction with PRESENILIN protein [38-40]. In rat brains, stabilisation of HIF-1α under hypoxia, fails with age [41]. To observe how age and the two different mutant alleles of *psen1* affect HIF-1α stabilisation in zebrafish brains, we used an antibody previously shown to detect a zebrafish paralogue of human HIF-1α, named Hif-1ab [42], to probe young and aged mutant and wild type sibling brains under normoxia and acute hypoxia (as described above and in Methods) (Figure 4). Under hypoxia, an age-related failure to stabilise Hif1ab over basal levels was obvious at 24 months of age, demonstrating that this is a phenomenon conserved between widely-diverged vertebrate brains. Interestingly, heterozygosity for the *psen1* fAD-like mutant alleles had no effect on Hif-1ab stabilisation in young adult brains. However, given the decreased Hif-1ab levels in aged fish with either mutant, the *Q96_K97del* allele (that preserves the open reading frame and should produce a full-length protein) caused the unexpected stabilisation of Hif1ab in aged brains (Figure 4B), while the coding sequence-truncating *K97fs* allele did not (Figure 4A). Further investigation of the age-dependent changes in the interaction between Hif1ab and the zebrafish Presenilin proteins (both wild type and mutant forms) may illuminate the mechanism underlying age-dependent failure of

HIF1α stabilisation and explain its unexpected stabilisation in the presence of a fAD-like mutant form of Psen1 only when it preserves the open reading frame.

Loss of PSEN1 expression is observed in human fAD brain tissue

To examine whether allelic bias might exist for fAD alleles of *PSEN1* in human carriers, we analysed wild type and mutant allele expression in three carriers of different *PSEN1* fAD mutations (see methods for details) in a region of the brain that shows typical AD histopathology (Aβ plaques and neurofibrillary tangles) with mild neuronal loss [43]. Total RNA was purified from the middle temporal gyrus of post-mortem brains of fAD mutation carriers and age-matched, cognitively normal controls, followed by cDNA synthesis and allele-specific dqPCR to analyse *PSEN1* wild type and mutant allele expression.

We did not observe a bias towards mutant allele expression in the three different mutation carriers. However, we saw a dramatic decrease in wild-type *PSEN1* allele expression in the three different mutation carriers compared to age-matched, cognitively normal controls (see Figure 5A-C). To confirm that the low levels of *PSEN1* transcripts in the deceased fAD carrier brains were not due to a generalised degradation of RNA, we normalised the wild type and mutant *PSEN1* allele measurements to the transcript levels from two, stably expressed reference genes, *cytochrome C1* (*CYC1)* and *ribosomal protein large 13 (RPL13)[44]* (see supp data 1). As expected, this did not alter the differences in *PSEN1* expression observed between mutation carriers versus controls.

A loss of function of one allele can be ameliorated by enhanced transcription of related DNA sequences in a process termed genetic compensation (reviewed in [45]). Therefore, we checked whether the functionally- and structurally-related human *PSEN2* gene was upregulated to compensate for the observed decrease in *PSEN1* in the fAD mutation carrier brains. We observed no upregulation of *PSEN2* in the mutation carriers compared to age-matched, cognitively normal controls (Figure 5D) and as was observed for *PSEN1*, *PSEN2* transcript levels were reduced in fAD brains relative to age-matched controls. (It should be highlighted that copy numbers for *PSEN2* were below the desired minimum threshold of 200 copies/µl for all samples, indicating that we observed low *PSEN2* expression in this brain region compared to other reports [46].) The possibility exists that the expression of the mutant allele in the *PSEN1* fAD mutation carriers is increased at earlier ages and stages of the disease followed by subsequent decreases at later stages of the disease. However, it is currently infeasible to test for this in living human brains. Our observation of loss of wild type *PSEN1* expression (with no apparent compensation by *PSEN2*) in human mutation carriers is consistent with a loss of normal PSEN1 function contributing to AD progression, although null alleles of *PSEN1* have never been identified in fAD.

Discussion

The production of energy supports all other cellular functions and is, therefore, fundamental to cellular, tissue, organ and organismal health. As the human brain ages, vascular function gradually degrades [21, 22] making it more difficult to deliver oxygen and energy substrates to support the brain's energy needs. As a consequence, transcription of *HIF1-α* is increased in the brain with age [47]. Increased HIF-1, acting to increase expression of *PDK1*, would be expected to increase the rate of

anaerobic glycolysis to maintain production of ATP (that is necessary, among other things, for maintaining the solubility of proteins to prevent the protein aggregation characteristic of neurodegenerative conditions [48]). However, a primary diagnostic marker of AD brains is that they are hypometabolic with both reduced oxygen and glucose consumption (as revealed by brain imaging studies, see review [21, 49]). Also, Liu *et al.* have found evidence for reduced levels of HIF1-α protein in post-mortem sporadic AD brains compared to normal, aged-matched controls [49]. These observations of human brain aging, our data on acceleration of aging in fAD-like mutants, and the hypoxia response data we have presented here, are consistent with a view of AD as both a normal possible outcome of aging and as a pathological, hypometabolic brain state. The data we have presented here are consistent with the "stress threshold change-of-state" model of AD progression we have previously presented [12]. This model postulates aged brains "inverting" (in terms of numerous molecular characteristics) into a pathological state as the brains reach homeostatic stress limits such as their limit to cope with the increasing oxidative stress resulting from increasing hypoxia. The clarity of the responses we have observed in whole zebrafish brains are due to our ability to place these entire (~10 mg) brains under acute hypoxia. The human brain is ~140,000-fold larger in mass than a zebrafish brain and the hypoxia it experiences as a result of failing vascular function would be expected to be regional (depending on energy demand and vascularisation) and to spread progressively as vascular function decreases.

While our observations are consistent with mutations in *PSEN* genes causing accelerated aging, there are numerous studies that question the idea of Alzheimer's disease being an inevitable consequence of age [50-52]. Even if the inverted

regulation of energy production under hypoxia we have observed in zebrafish is, in fact, related to the brain hypometabolism of Alzheimer's disease, this does not show that Alzheimer's disease is an inevitable consequence of aging. Rather, our results only support that age is a major risk factor for Alzheimer's disease and may even be a necessary precondition for the disease.

Our study has uncovered a number of phenomena that we currently cannot explain. Why is it that, under acute hypoxia, two year old zebrafish brains cannot stabilise Hif1ab but are still able to upregulate HRGs? Are there HIF-1-independent systems activating HRGs such as *PGC-1α* [53]? Why does heterozygosity for only the fAD-like mutation in *psen1* that does not truncate the open reading frame allow unexpected stabilisation of Hif1ab under hypoxia in aged zebrafish while upregulation of HRGs nevertheless fails? Indeed, why do transcript levels HRGs decrease under hypoxia in these fish rather than increasing or, at least, not changing? Clearly, neither age nor the presence of mutations in *psen1* alone is sufficient to explain these phenomena and an interaction between these two factors is involved. HIF1-α has been shown to interact with PRESENILIN 1 protein [38-40] to increase γ-secretase activity post-transcriptionally [40]. In turn, increased γ-secretase activity increases HIF1-α stability (and so HIF1 activity) via a p75NTR-dependent feed-forward mechanism [54]. Future work must investigate age-dependent changes in the interaction between HIF1 and the PRESENILINs and reveal the basis of the failure of HIF1-α stabilisation with advanced age. Delaying the onset of this failure might delay the onset of Alzheimer's disease. At present, physical exercise that maintains vascular health is one of the few potential protective treatments available for LOAD [55-58]. Indeed, a recent systematic review has revealed for the first time an association between physical

exercise and better cognitive outcomes at expected symptom onset in individuals with fAD [59].

HIF-1 is regarded as a central regulator of responses to hypoxia. However, remarkably, it also regulates genes involved in iron homeostasis (see review [32]). This raises the possibility that the increased expression of HIF-1-target genes in young *psen1* mutant brains may actually be due to decreased cytosolic Fe^{2+} availability (that stabilises HIF-1α) rather than hypoxia. Hypothetically, this situation might arise because correct acidification of the endo-lysosomal pathway is required for most iron importation and for recycling of the iron in damaged mitochondria and in ferritin into its Fe^{2+} form via autophagy (reviewed in [12]). fAD mutations in the *PRESENILIN*s apparently decrease lysosomal acidification [60] and this is predicted to decrease Fe^{2+} availability. Meanwhile, the fAD gene *APP* that encodes the protein precursor of the Aβ peptide, plays a role in iron export since full-length APP, (and at least one secreted form of APP, sAPPα), can stabilise Ferroportin to increase export of Fe^{2+} from neurons [61, 62]. These phenomena have led us to propose that fAD mutations in the *PSEN* genes and *APP* may share common roles in iron dyshomeostasis [12]. The increased expression of HIF-1-target genes we have observed in the brains of young adult zebrafish is consistent with this idea. Further testing will be required to verify whether or not iron dyshomeostasis actually exists in these young brains.

Biased expression of alleles in heterozygotes has been recognised for decades but has mainly been attributed to imprinting or differences in cis-regulatory sequences [63, 64]. Recently Huang et al [65] discovered widespread allele-specific expression in

mouse and primate brains including for a small number of autosomal genes that showed what they termed "antagonistic allele expression effects" where one allele appears expressed at the expense of another. Only a small proportion of this biased allele expression appeared to be due to imprinting. We observed that, for two very different forms of mutant *psen1* allele in heterozygous zebrafish brains, the expression from the mutant allele (during both aging and under acute hypoxic stress) increases at the apparent expense of the wild type allele. This strongly supports that changes in the expression of specific *psen1* alleles are occurring within heterozygous cells and not between cells (i.e. they are not due to changes in any proportion of maternally and, or paternally imprinted cells). Future single cell RNAseq analyses should give us information on the uniformity of the bias in *psen1* allele expression between cells [66].

Our mutant zebrafish were generated using an inbred strain, and any breeding of mutants has been conducted within that inbred strain. Therefore, allele-specific expression differences due to differences in cis-regulatory sequences are unlikely. We have previously observed remarkable homeostasis of Psen1 protein levels in zebrafish embryos, apparently by a mechanism that responds to levels of full-length Psen1 protein to feed back onto regulation of *psen1* gene transcription [67]. However, in the *K97fs* mutation heterozygotes, there is an increase in mutant transcript levels with age and under stress despite that this allele's open reading frame is truncated. Since the *PSEN* genes are involved in regulating the unfolded protein response [27, 31, 68], (a stress response that includes regulation of mRNA stability [69, 70]), it is conceivable that the allele-specific changes in *psen1* mRNA level reflect changes in RNA stability rather than changes in the rate of transcription initiation. It may be possible to

distinguish between these two mechanisms by comparison of changes in mRNA versus nascent transcript levels using PCRs specific for spliced and un-spliced transcripts [67].

While we did not observe bias in allele expression in bulk samples of middle temporal gyrus from carriers of three different *PSEN1* fAD mutations, we did observe severe loss of *PSEN1* transcript expression. If this phenomenon is widespread in LOAD brains, then loss of normal *PSEN1* function could be important in Alzheimer's disease pathogenesis. However, the published expression data for *PSEN1* in human LOAD brain tissue shows varying results depending on the brain region studied, the method of measurement, and which particular splice variant is measured. For example, in LOAD brains, a decrease in expression of *PSEN1* mRNA has been observed in the hippocampus (along with *PSEN2*) [71] and in the frontotemporal region [72] while an increase in expression of *PSEN1* mRNA has been measured in the temporal lobes [73, 74] and superior frontal gyrus [74]. Other studies reported no significant difference in *PSEN1* expression in LOAD in the frontal cortex [75, 76], the entorhinal cortex, the auditory cortex (although decreased *PSEN2* was observed) or the hippocampus [77]. It is difficult to form any firm conclusions on *PSEN1* mRNA expression in LOAD from these inconsistent findings and this should encourage more detailed analysis of *PSEN1* expression in both fAD and LOAD brains in the future.

Methods

Zebrafish husbandry and animal ethics

Tubingen-strain zebrafish were maintained in a recirculated water system. All work with zebrafish was conducted under the auspices of the Animal Ethics Committee of

the University of Adelaide (permit no. 31945) and Institutional Biosafety Committee (IBC Dealing ID 122210).

Production of the psen1 mutations

Production of the *psen*^{K97fs} mutation was previously described in *Hin et al, 2018 submitted*. During the screening of individual zebrafish for the desired *psen*^{K97fs} mutation, a second mutation was identified at the same site, a deletion of 6 nucleotides, CAGAAG, which is an in-frame deletion of 2 codons, *psen1*$^{Q96\_K97del}$.

Genomic DNA extraction and genotyping PCR of zebrafish tissue

DNA was extracted from adult zebrafish tail clips and genotyped via PCR as described in *Hin et al, 2018 submitted*. Primers used for genotyping PCR were synthesized by Sigma-Aldrich. Oligonucleotide sequences are given in Table 2.

Whole brain removal from adult zebrafish

Adult fish were euthanized by sudden immersion in an ice water slurry for at least 30 seconds before immediate decapitation. The entire brain was then removed from the cranium for immediate RNA or protein extraction. All fish brains were sampled at late morning/noon to minimise effects of circadian rhythms.

Hypoxia treatment of adult zebrafish

Male or female adult zebrafish at the desired age and genotype were treated in low oxygen levels by placing zebrafish in oxygen-depleted water for 3 hours (oxygen concentration of 6.6 ± 0.5 mg/L in normoxia and 1.1 ± 0.5mg/L in hypoxia [23]. Brains were subsequently used for digital PCR or western blotting analysis.

RNA extraction and cDNA synthesis of total adult zebrafish brain

Total RNA was extracted from whole zebrafish brain (~10mg) using the QIAGEN RNeasy Mini Kit according to the manufacture's protocol as described in [23, 31]. The RNA was DNase treated using RQ1 DNase from Promega according to the manufacturer's instructions. RNA was quantified using a Nanodrop spectrophotometer. cDNA was synthesized using random hexamers and Superscript III First Strand Synthesis System (Thermo Fisher) according to the manufacturer's instructions.

RNA extraction and cDNA synthesis from human brain tissue

Human brain tissues were obtained from the Sydney Brain Bank at Neuroscience Research Australia and the NSW Tissue Resource Centre at the University of Sydney. The brains were collected under institutional ethics approvals. Whole brains were sliced into blocks and fresh-frozen and stored at -80°C. Tissue samples from three cases with mutant *PSEN1* and three age- and gender-matched controls (see Table 1 for details without significant neuropathology were processed for RNA extraction using TRIzol reagent (Invitrogen) following the manufacturer's protocol. All procedures were carried out using RNase-free reagents and consumables. Five micrograms of RNA was reverse transcribed into cDNA using Moloney-murine leukemia virus reverse transcriptase and random primers (Promega, Madison, Wisconsin, USA) in 20 µl reaction volume. RNA integrity was assessed with high resolution capillary electrophoresis (Agilent Technologies) and only RNA with RNA Integrity Number (RIN) value greater than 6.0 was used.

3D Quant Studio Digital PCR

Digital PCR was performed on a QuantStudio™ 3D Digital PCR System (Life Technologies). Reaction mixes contained 1X QuantStudio™3D digital PCR Master Mix, Sybr® dye, 200nM of specific primers and 12.5 - 500ng cDNA (500ng for *PSEN1* and *PSEN2*, 100ng for *CYC1* and *RPL13*, 50ng for *cd44a*, *edn1*, *igfbp3*, 25ng for *psen1* and *pdk1* and 12.5 ng for *mmp2*). The reaction mixture (14.5µl) was loaded onto a QuantStudio™3D digital PCR 20 K chip using an automatic chip loader according to the manufacturer's instructions. Loaded chips underwent thermo-cycling on the Gene Amp 9700 thermo-cycling system under the following conditions: 96°C for 10 min, 39 cycles of 60°C (59°C for *CYC1* and *PSEN1*G206Vsite) for 2 min and 98°C for 30 sec, followed by a final extension step at 60°C (or 59°C see above) for 2 min. The chips were imaged on a QuantStudio™ 3D instrument, which assesses raw data and calculates the estimated concentration of the nucleic acid sequence targeted by the Sybr® dye by Poisson distribution [78]. Primers used were synthesized by Sigma-Aldrich and are listed in Table 2.

Protein extraction of total adult zebrafish brain

Each brain was homogenised in water supplemented with reducing agent (Thermo Fisher Scientific) and complete protease inhibitors (Roche Life Sciences), LDS buffer (Thermo Fisher Scientific) was then added and the sample was briefly homogenised and placed at 90°C for 20 minutes. Each sample was aliquoted. To generate a protein standard to allow quantitative comparison between signals on separate western blots, 8 male non-mutant adult zebrafish at 6 months of age were selected and placed under hypoxia as described in [23]. Protein was extracted from each brain as above. After extraction all homogenates were combined, thoroughly mixed and aliquoted, with one

aliquot being sufficient for one western blot. All samples and standards were stored at -80°C until required.

Protein Immunoblotting

Samples and standards were prepared by sonication for 10 minutes followed by incubation at 90°C for 5 minutes. PrecisionPlusProteinDualXtra ladder (Bio-Rad) (7µl), standards (3 x 10µl) and samples (6 x ~18µl) were loaded on a 4-12% Bis-Tris Nu-PAGE (Life Technologies) gel for electrophoresis. The protein samples and standards were subsequently transferred to a PVDF membrane using the Mini Blot Module transfer system according to the manufacturer's protocol (Thermo Fisher Scientific). To detect the Hif1ab protein, the membrane was initially blocked in 3% skim milk followed by incubation in a 1/3000 dilution of the Hif1ab antibody (Gene Tex, cat no. GTX131826). The membrane was washed and incubated in a 1/2500 dilution of the rabbit-HRP secondary antibody (Sigma). After washing, Hif1ab protein was detected on the membrane using ECL detection reagents (Thermo Fisher Scientific) and visualised using the Chemi Doc Imaging System (Bio-Rad). The Hif1ab protein band can be visualised at ~100kDa. Using Image Lab software (Bio-Rad), densitometry analysis was performed for the Hif1ab protein band for each sample and standard. An average value was obtained for the standards for each membrane. Each sample value was then normalised to the average standard value. Each protein sample was quantified using the EZQ protein quantification kit (Thermo Fisher Scientific) according to the manufacturer's protocol. The standard normalised value for each sample was then expressed as Hif1ab per total protein loaded. Each membrane displayed 3 normoxia and 3 hypoxia samples from the same age (6 or 24

months) and the same genotype (+/+, *psen1*$^{Q96\_K97del}$/+ or *psen1*^{K97fs}/+) together with the protein standard in separate 3 wells.

L-Lactate Content Analysis of zebrafish brain

L-Lactate content was analysed using the Lactate Colorimetric Kit II (BioVision). Brains were removed from zebrafish adults in cold 1xPBS, then weighed and homogenized in the Lactate Assay Buffer provided in the kit. Each sample was then filtered through a 10kDa MW spin filter (Sartorius Stedium Biotech) to remove all proteins. The lactate content of the eluate from each zebrafish brain was determined using the kit according to the manufacturer's protocol and the original brain weight was used to calculate the nmol of lactate per mg of brain tissue.

***PSEN1* mutation**	**Codon change**	**Gender**	**Age at death (years)**	**Disease duration (years)**	**PMD (hours)**	**Project ID**
L271V	CTG to GTG	Female	51	5	5	LA1
L219P	CTT to CCT	Female	61	7	13	LA2
G206V	GGT to GTT	Female	32	3	22	LA3
Control (L271V)	N/A	Female	51	N/A	41	LC2
Control (L219P)	N/A	Female	60	N/A	41	LC1
Control (G206V)	N/A	Female	29	N/A	40	LC3

Table 1. Human *PSEN1* mutations analysed for allele-specific dqPCR including age-matched control details. Post-mortem delay (PMD).

Gene symbol	**Accession number**	**Target allele binding site**	**Sense primer (5'→3')**	**Anti-sense primer (5'→3')**
Genotyping (genomic DNA)				
psen1	ENSDARG00000004870	***WT (K97 site)***	TCTGTCAGCTTCTACACACAGAAGG	AGTAGGAGCAGTTTAGGGATGG
psen1	ENSDARG00000004870	***GAdel (K97fs)***	AATCTGTCAGCTTCTACACACAAGG	AGTAGGAGCAGTTTAGGGATGG
psen1	ENSDARG00000004870	***CAGAAGdel (Q96_K97del)***	TGTCAGCTTCTACACAGACGGA	AGTAGGAGCAGTTTAGGGATGG
psen1	ENSDARG00000004870	***WT (exon 4-intron)***	GGCACACAAGCAGCACCG	TCCTTTCCTGTCATTCAGACCTGCGA
psen1	ENSDARG00000004870	***WT-sequencing***	AGCCGTAATGAGGTGGAGC	N/A
dqPCR (cDNA)				
psen1	NM_131024	***WT (K97 site)***	CTACACACAGAAGGACGGACAGC	GCCAGGCTTGAATCACCTTGTA
psen1	NM_131024	***GAdel (K97fs)***	TCTGTCAGCTTCTACACACAAGGA	GCCAGGCTTGAATCACCTTGTA
psen1	NM_131024	***CAGAAGdel (Q96_K97del)***	CTACACAGACGGACAGCAGCTG	GCCAGGCTTGAATCACCTTGTA
PSEN1	NM_000021.3	***WT (L271 site)***	CATTACTGTTGCACTCCTGATC	CTCCTGAGCTGTTTCAACCAG
PSEN1	NM_000021.3	***L271V mutation***	CATTACTGTTGCACTCCTGATC	CTCCTGAGCTGTTTCAACCAC
PSEN1	NM_000021.3	***WT (L219 site)***	CATTACTGTTGCACTCCTGATC	ATGCCTGCTGGAGTCGAA
PSEN1	NM_000021.3	***L219P mutation***	CATTACTGTTGCACTCCTGATC	GCCTGCTGGAGTCGAGG

PSEN1	NM_000021.3	***WT (G206 site)***	GGTCATCCATGCCTGGC	GGAAATCATTCCCACCACAC
PSEN1	NM_000021.3	***G206V mutation***	GGTCATCCATGCCTGGC	GGAAATCATTCCCACCACAA
PSEN2	NM_012486.2	***WT***	CATGATCGTGGTGGTAGCC	GGATGAACTTGTAGCAGCGG
CYC1	NM_001916	***WT***	AGCCTACAAGAAAGTTTGCCTAT	TCTTCTTCCGGTAGTGGATCTTGGC
RPL13	NM_00977	***WT***	CCTGGAGGAGAAGAGGAAAGAGA	TTGAGGACCTCTGTGTATTTGTCAA
cd44a	XM_001922456	***WT***	CCCATCAGATTCATCACCAAACT	AGAATGAACTGTCTCTGGCTGC
edn1	NM_131519	***WT***	CGTTACAGTTTAAAGCAGCGTCA	TGTGTTTGCATTGCTTCCCAG
mmp2	NM_198067	***WT***	CCTGAGACAGCAATGTCAACATCA	CATCATTGCGCCCTGATGTG
igfbp3	NM_205751	***WT***	AGTGCAGTCCATCCATCCAAAGGC	GTCTCCATGTTATAGCAGTGGACCT
pdk1	XM_678484	***WT***	ACAACCTGAATATAGTCTTAGC	GTGTGGAGTGTGATGATG

Table 2. Primer sequences for genotyping, sequencing and dqPCR. WT denotes wild type allele-specific PCR. The WT primer target site for *psen1* or *PSEN1* is indicated in parentheses.

Acknowledgements

This research was supported by a grant from Australia's National Health and Medical Research Council (NHMRC), (#1126422). MN was also generously supported by a grant from the family of Lindsay Carthew.

Brain tissues were received from the Sydney Brain Bank at Neuroscience Research Australia, which is supported by The University of New South Wales and Neuroscience Research Australia. G.M.H. is a National Health and Medical Research Council of Australia Senior Principal Research Fellow (#1079679). Tissues were processed in the Dementia and Movement Disorders Laboratory supported by Forefront, a collaborative research group dedicated to the study of non-Alzheimer disease degenerative disorders, funded by NHMRC grants (#1037746 and #1095127).

Competing Interests

Nothing to disclose

References

1. Mawuenyega KG, Sigurdson W, Ovod V, Munsell L, Kasten T, Morris JC, et al. Decreased clearance of CNS beta-amyloid in Alzheimer's disease. Science. 2010;330(6012):1774. doi: 10.1126/science.1197623. PubMed PMID: 21148344; PubMed Central PMCID: PMC3073454.
2. Villemagne VL, Burnham S, Bourgeat P, Brown B, Ellis KA, Salvado O, et al. Amyloid beta deposition, neurodegeneration, and cognitive decline in sporadic Alzheimer's disease: a prospective cohort study. Lancet Neurol. 2013;12(4):357-67. Epub 2013/03/13. doi: 10.1016/S1474-4422(13)70044-9. PubMed PMID: 23477989.
3. Bateman RJ, Xiong C, Benzinger TL, Fagan AM, Goate A, Fox NC, et al. Clinical and biomarker changes in dominantly inherited Alzheimer's disease. N Engl J Med. 2012;367(9):795-804. doi: 10.1056/NEJMoa1202753. PubMed PMID: 22784036; PubMed Central PMCID: PMC3474597.
4. Iturria-Medina Y, Sotero RC, Toussaint PJ, Mateos-Perez JM, Evans AC, Alzheimer's Disease Neuroimaging I. Early role of vascular dysregulation on late-onset Alzheimer's disease based on multifactorial data-driven analysis. Nat Commun.

2016;7:11934. doi: 10.1038/ncomms11934. PubMed PMID: 27327500; PubMed Central PMCID: PMC4919512.
5. Karran E, De Strooper B. The amyloid cascade hypothesis: are we poised for success or failure? J Neurochem. 2016;139 Suppl 2:237-52. Epub 2016/11/01. doi: 10.1111/jnc.13632. PubMed PMID: 27255958.
6. Doig AJ, Del Castillo-Frias MP, Berthoumieu O, Tarus B, Nasica-Labouze J, Sterpone F, et al. Why Is Research on Amyloid-beta Failing to Give New Drugs for Alzheimer's Disease? ACS Chem Neurosci. 2017;8(7):1435-7. Epub 2017/06/07. doi: 10.1021/acschemneuro.7b00188. PubMed PMID: 28586203.
7. Guerreiro R, Hardy J. Genetics of Alzheimer's disease. Neurotherapeutics : the journal of the American Society for Experimental NeuroTherapeutics. 2014;11(4):732-7. PubMed PMID: Medline:25113539.
8. Jayadev S, Leverenz JB, Steinbart E, Stahl J, Klunk W, Yu CE, et al. Alzheimer's disease phenotypes and genotypes associated with mutations in presenilin 2. Brain. 2010;133:1143-54. doi: Doi 10.1093/Brain/Awq033. PubMed PMID: ISI:000277225600017.
9. Masters CL, Bateman RJ, Blennow K, Rowe CC, Sperling RA, Cummings JL. Alzheimer's disease. Nature reviews Disease Primers. 2015;1:1-8. doi: doi:10.1038/nrdp.2015.56.
10. Pottier C, Hannequin D, Coutant S, Rovelet-Lecrux A, Wallon D, Rousseau S, et al. High frequency of potentially pathogenic SORL1 mutations in autosomal dominant early-onset Alzheimer disease. Mol Psychiatry. 2012;17(9):875-9. Epub 2012/04/05. doi: 10.1038/mp.2012.15. PubMed PMID: 22472873.
11. Jayne T, Newman M, Verdile G, Sutherland G, Munch G, Musgrave I, et al. Evidence For and Against a Pathogenic Role of Reduced gamma-Secretase Activity in Familial Alzheimer's Disease. Journal of Alzheimer's disease : JAD. 2016;52(3):781-99. doi: 10.3233/JAD-151186. PubMed PMID: 27060961.
12. Lumsden AL, Rogers JT, Majd S, Newman M, Sutherland GT, Verdile G, et al. Dysregulation of Neuronal Iron Homeostasis as an Alternative Unifying Effect of Mutations Causing Familial Alzheimer's Disease. Front Neurosci. 2018;12:533. Epub 2018/08/29. doi: 10.3389/fnins.2018.00533. PubMed PMID: 30150923; PubMed Central PMCID: PMCPMC6099262.
13. Quiroz YT, Schultz AP, Chen K, Protas HD, Brickhouse M, Fleisher AS, et al. Brain Imaging and Blood Biomarker Abnormalities in Children With Autosomal Dominant Alzheimer Disease: A Cross-Sectional Study. JAMA Neurol. 2015;72(8):912-9. doi: 10.1001/jamaneurol.2015.1099. PubMed PMID: 26121081; PubMed Central PMCID: PMC4625544.
14. Reiman EM, Quiroz YT, Fleisher AS, Chen K, Velez-Pardo C, Jimenez-Del-Rio M, et al. Brain imaging and fluid biomarker analysis in young adults at genetic risk for autosomal dominant Alzheimer's disease in the presenilin 1 E280A kindred: a case-control study. Lancet Neurol. 2012;11(12):1048-56. doi: 10.1016/S1474-4422(12)70228-4. PubMed PMID: 23137948; PubMed Central PMCID: PMC4181671.
15. Gordon BA, Blazey TM, Su Y, Hari-Raj A, Dincer A, Flores S, et al. Spatial patterns of neuroimaging biomarker change in individuals from families with autosomal dominant Alzheimer's disease: a longitudinal study. The Lancet Neurology. 2018;17(3):241-50. doi: https://doi.org/10.1016/S1474-4422(18)30028-0.
16. de Bruijn RF, Ikram MA. Cardiovascular risk factors and future risk of Alzheimer's disease. BMC medicine. 2014;12:130. Epub 2014/11/12. doi:

10.1186/s12916-014-0130-5. PubMed PMID: 25385322; PubMed Central PMCID: PMC4226863.
17. O'Brien JT, Markus HS. Vascular risk factors and Alzheimer's disease. BMC medicine. 2014;12:218. Epub 2014/11/12. doi: 10.1186/s12916-014-0218-y. PubMed PMID: 25385509; PubMed Central PMCID: PMCPMC4226870.
18. Reitz C, Mayeux R. Alzheimer disease: epidemiology, diagnostic criteria, risk factors and biomarkers. Biochem Pharmacol. 2014;88(4):640-51. Epub 2014/01/09. doi: 10.1016/j.bcp.2013.12.024. PubMed PMID: 24398425; PubMed Central PMCID: PMCPMC3992261.
19. Panza GA, Taylor BA, MacDonald HV, Johnson BT, Zaleski AL, Livingston J, et al. Can Exercise Improve Cognitive Symptoms of Alzheimer's Disease? A Meta-Analysis. J Am Geriatr Soc. 2018. doi: 10.1111/jgs.15241. PubMed PMID: 29363108.
20. Kirk-Sanchez NJ, McGough EL. Physical exercise and cognitive performance in the elderly: current perspectives. Clin Interv Aging. 2014;9:51-62. doi: 10.2147/CIA.S39506. PubMed PMID: 24379659; PubMed Central PMCID: PMC3872007.
21. Daulatzai MA. Cerebral hypoperfusion and glucose hypometabolism: Key pathophysiological modulators promote neurodegeneration, cognitive impairment, and Alzheimer's disease. J Neurosci Res. 2017;95(4):943-72. doi: 10.1002/jnr.23777. PubMed PMID: 27350397.
22. Crawford JG. Alzheimer's disease risk factors as related to cerebral blood flow. Med Hypotheses. 1996;46(4):367-77. Epub 1996/04/01. PubMed PMID: 8733167.
23. Moussavi Nik SH, Wilson L, Newman M, Croft K, Mori TA, Musgrave I, et al. The BACE1-PSEN-AbetaPP regulatory axis has an ancient role in response to low oxygen/oxidative stress. Journal of Alzheimer's disease : JAD. 2012;28(3):515-30. Epub 2011/11/03. doi: V37W532375G50726 [pii] 10.3233/JAD-2011-110533. PubMed PMID: 22045484.
24. Lukiw WJ, Gordon WC, Rogaev EI, Thompson H, Bazan NG. Presenilin-2 (PS2) expression up-regulation in a model of retinopathy of prematurity and pathoangiogenesis. Neuroreport. 2001;12(1):53-7. PubMed PMID: 11201091.
25. Oresic M, Hyotylainen T, Herukka SK, Sysi-Aho M, Mattila I, Seppanan-Laakso T, et al. Metabolome in progression to Alzheimer's disease. Transl Psychiatry. 2011;1:e57. Epub 2011/01/01. doi: 10.1038/tp.2011.55. PubMed PMID: 22832349; PubMed Central PMCID: PMC3309497.
26. Manabe T, Katayama T, Sato N, Gomi F, Hitomi J, Yanagita T, et al. Induced HMGA1a expression causes aberrant splicing of Presenilin-2 pre-mRNA in sporadic Alzheimer's disease. Cell Death and Differentiation. 2003;10(6):698-708. doi: DOI 10.1038/sj.cdd.4401221. PubMed PMID: ISI:000183299200009.
27. Sato N, Imaizumi K, Manabe T, Taniguchi M, Hitomi J, Katayama T, et al. Increased production of beta-amyloid and vulnerability to endoplasmic reticulum stress by an aberrant spliced form of presenilin 2. Journal of Biological Chemistry. 2001;276(3):2108-14. PubMed PMID: ISI:000166528000063.
28. Manabe T, Katayama T, Sato N, Kudo T, Matsuzaki S, Imaizumi K, et al. The cytosolic inclusion bodies that consist of splice variants that lack exon 5 of the presenilin-2 gene differ obviously from Hirano bodies observed in the brain from sporadic cases of Alzheimer's disease patients. Neuroscience letters. 2002;328(2):198-200. PubMed PMID: ISI:000177520600029.

29. Cruts M, Theuns J, Van Broeckhoven C. Locus-specific mutation databases for neurodegenerative brain diseases. Hum Mutat. 2012;33(9):1340-4. doi: 10.1002/humu.22117. PubMed PMID: 22581678; PubMed Central PMCID: PMC3465795.
30. Zhang X, Le W. Pathological role of hypoxia in Alzheimer's disease. Exp Neurol. 2010;223(2):299-303. doi: 10.1016/j.expneurol.2009.07.033. PubMed PMID: 19679125.
31. Moussavi Nik SH, Newman M, Wilson L, Ebrahimie E, Wells S, Musgrave I, et al. Alzheimer's disease-related peptide PS2V plays ancient, conserved roles in suppression of the unfolded protein response under hypoxia and stimulation of gamma-secretase activity. Hum Mol Genet. 2015. Epub 2015/03/31. doi: 10.1093/hmg/ddv110. PubMed PMID: 25814654.
32. Harris AL. Hypoxia--a key regulatory factor in tumour growth. Nature reviews Cancer. 2002;2(1):38-47. Epub 2002/03/21. doi: 10.1038/nrc704. PubMed PMID: 11902584.
33. Kim JW, Tchernyshyov I, Semenza GL, Dang CV. HIF-1-mediated expression of pyruvate dehydrogenase kinase: a metabolic switch required for cellular adaptation to hypoxia. Cell Metab. 2006;3(3):177-85. doi: 10.1016/j.cmet.2006.02.002. PubMed PMID: 16517405.
34. Paolicchi E, Gemignani F, Krstic-Demonacos M, Dedhar S, Mutti L, Landi S. Targeting hypoxic response for cancer therapy. Oncotarget. 2016;7(12):13464-78. Epub 2016/02/10. doi: 10.18632/oncotarget.7229. PubMed PMID: 26859576; PubMed Central PMCID: PMCPMC4924654.
35. Kuang X, Liu C, Fang J, Ma W, Zhang J, Cui S. The tumor suppressor gene lkb1 is essential for glucose homeostasis during zebrafish early development. FEBS Lett. 2016;590(14):2076-85. Epub 2016/06/07. doi: 10.1002/1873-3468.12237. PubMed PMID: 27264935.
36. Caceda R, Gamboa JL, Boero JA, Monge CC, Arregui A. Energetic metabolism in mouse cerebral cortex during chronic hypoxia. Neuroscience letters. 2001;301(3):171-4. Epub 2001/03/21. PubMed PMID: 11257425.
37. Gerhard GS, Kauffman EJ, Wang X, Stewart R, Moore JL, Kasales CJ, et al. Life spans and senescent phenotypes in two strains of Zebrafish (Danio rerio). Experimental gerontology. 2002;37(8-9):1055-68. Epub 2002/09/06. PubMed PMID: 12213556.
38. De Gasperi R, Sosa MA, Dracheva S, Elder GA. Presenilin-1 regulates induction of hypoxia inducible factor-1alpha: altered activation by a mutation associated with familial Alzheimer's disease. Mol Neurodegener. 2010;5:38. doi: 10.1186/1750-1326-5-38. PubMed PMID: 20863403; PubMed Central PMCID: PMC2955646.
39. Kaufmann MR, Barth S, Konietzko U, Wu B, Egger S, Kunze R, et al. Dysregulation of hypoxia-inducible factor by presenilin/gamma-secretase loss-of-function mutations. J Neurosci. 2013;33(5):1915-26. Epub 2013/02/01. doi: 10.1523/JNEUROSCI.3402-12.2013. PubMed PMID: 23365231.
40. Villa JC, Chiu D, Brandes AH, Escorcia FE, Villa CH, Maguire WF, et al. Nontranscriptional role of Hif-1alpha in activation of gamma-secretase and notch signaling in breast cancer. Cell Rep. 2014;8(4):1077-92. Epub 2014/08/19. doi: 10.1016/j.celrep.2014.07.028. PubMed PMID: 25131208.
41. Ndubuizu OI, Chavez JC, LaManna JC. Increased prolyl 4-hydroxylase expression and differential regulation of hypoxia-inducible factors in the aged rat brain. Am J Physiol Regul Integr Comp Physiol. 2009;297(1):R158-65. doi:

10.1152/ajpregu.90829.2008. PubMed PMID: 19420289; PubMed Central PMCID: PMC2711700.
42. Liu S, Zhu K, Chen N, Wang W, Wang H. Identification of HIF-1alpha promoter and expression regulation of HIF-1alpha gene by LPS and hypoxia in zebrafish. Fish physiology and biochemistry. 2013;39(5):1153-63. Epub 2013/02/09. doi: 10.1007/s10695-013-9771-0. PubMed PMID: 23392835.
43. Mountjoy CQ, Roth M, Evans NJ, Evans HM. Cortical neuronal counts in normal elderly controls and demented patients. Neurobiology of aging. 1983;4(1):1-11. Epub 1983/01/01. PubMed PMID: 6877482.
44. Rydbirk R, Folke J, Winge K, Aznar S, Pakkenberg B, Brudek T. Assessment of brain reference genes for RT-qPCR studies in neurodegenerative diseases. Sci Rep-Uk. 2016;6. doi: ARTN 37116
10.1038/srep37116. PubMed PMID: WOS:000388152100001.
45. El-Brolosy MA, Stainier DYR. Genetic compensation: A phenomenon in search of mechanisms. PLoS Genet. 2017;13(7):e1006780. Epub 2017/07/14. doi: 10.1371/journal.pgen.1006780. PubMed PMID: 28704371; PubMed Central PMCID: PMCPMC5509088.
46. Hawrylycz MJ, Lein ES, Guillozet-Bongaarts AL, Shen EH, Ng L, Miller JA, et al. An anatomically comprehensive atlas of the adult human brain transcriptome. Nature. 2012;489(7416):391-9. Epub 2012/09/22. doi: 10.1038/nature11405. PubMed PMID: 22996553; PubMed Central PMCID: PMCPMC4243026.
47. Lu T, Pan Y, Kao SY, Li C, Kohane I, Chan J, et al. Gene regulation and DNA damage in the ageing human brain. Nature. 2004;429(6994):883-91. doi: 10.1038/nature02661. PubMed PMID: 15190254.
48. Patel A, Malinovska L, Saha S, Wang J, Alberti S, Krishnan Y, et al. ATP as a biological hydrotrope. Science. 2017;356(6339):753-6. doi: 10.1126/science.aaf6846. PubMed PMID: 28522535.
49. Liu Y, Liu F, Iqbal K, Grundke-Iqbal I, Gong CX. Decreased glucose transporters correlate to abnormal hyperphosphorylation of tau in Alzheimer disease. FEBS Lett. 2008;582(2):359-64. doi: 10.1016/j.febslet.2007.12.035. PubMed PMID: 18174027; PubMed Central PMCID: PMC2247364.
50. Qiu C, Fratiglioni L. Aging without Dementia is Achievable: Current Evidence from Epidemiological Research. Journal of Alzheimer's disease : JAD. 2018;62(3):933-42. Epub 2018/03/23. doi: 10.3233/JAD-171037. PubMed PMID: 29562544; PubMed Central PMCID: PMCPMC5870011.
51. Boeve B, McCormick J, Smith G, Ferman T, Rummans T, Carpenter T, et al. Mild cognitive impairment in the oldest old. Neurology. 2003;60(3):477-80. Epub 2003/02/13. PubMed PMID: 12578930.
52. Andersen-Ranberg K, Vasegaard L, Jeune B. Dementia is not inevitable: a population-based study of Danish centenarians. J Gerontol B Psychol Sci Soc Sci. 2001;56(3):P152-9. Epub 2001/04/24. PubMed PMID: 11316833.
53. Ndubuizu OI, Tsipis CP, Li A, LaManna JC. Hypoxia-inducible factor-1 (HIF-1)-independent microvascular angiogenesis in the aged rat brain. Brain Res. 2010;1366:101-9. Epub 2010/09/30. doi: 10.1016/j.brainres.2010.09.064. PubMed PMID: 20875806; PubMed Central PMCID: PMCPMC3378376.
54. Le Moan N, Houslay DM, Christian F, Houslay MD, Akassoglou K. Oxygen-dependent cleavage of the p75 neurotrophin receptor triggers stabilization of HIF-1alpha. Molecular cell. 2011;44(3):476-90. Epub 2011/11/08. doi: 10.1016/j.molcel.2011.08.033. PubMed PMID: 22055192; PubMed Central PMCID: PMCPMC3212815.

55. Santos-Lozano A, Pareja-Galeano H, Sanchis-Gomar F, Quindos-Rubial M, Fiuza-Luces C, Cristi-Montero C, et al. Physical Activity and Alzheimer Disease: A Protective Association. Mayo Clinic proceedings. 2016;91(8):999-1020. Epub 2016/08/06. doi: 10.1016/j.mayocp.2016.04.024. PubMed PMID: 27492909.
56. Stephen R, Hongisto K, Solomon A, Lonnroos E. Physical Activity and Alzheimer's Disease: A Systematic Review. The journals of gerontology Series A, Biological sciences and medical sciences. 2017;72(6):733-9. Epub 2017/01/05. doi: 10.1093/gerona/glw251. PubMed PMID: 28049634.
57. Beydoun MA, Beydoun HA, Gamaldo AA, Teel A, Zonderman AB, Wang Y. Epidemiologic studies of modifiable factors associated with cognition and dementia: systematic review and meta-analysis. BMC public health. 2014;14:643. Epub 2014/06/26. doi: 10.1186/1471-2458-14-643. PubMed PMID: 24962204; PubMed Central PMCID: PMCPMC4099157.
58. Frederiksen KS, Gjerum L, Waldemar G, Hasselbalch SG. Effects of Physical Exercise on Alzheimer's Disease Biomarkers: A Systematic Review of Intervention Studies. Journal of Alzheimer's disease : JAD. 2018;61(1):359-72. Epub 2017/11/21. doi: 10.3233/jad-170567. PubMed PMID: 29154278.
59. Muller S, Preische O, Sohrabi HR, Graber S, Jucker M, Ringman JM, et al. Relationship between physical activity, cognition, and Alzheimer pathology in autosomal dominant Alzheimer's disease. Alzheimer's & dementia : the journal of the Alzheimer's Association. 2018. Epub 2018/09/30. doi: 10.1016/j.jalz.2018.06.3059. PubMed PMID: 30266303.
60. Lee JH, Yu WH, Kumar A, Lee S, Mohan PS, Peterhoff CM, et al. Lysosomal proteolysis and autophagy require presenilin 1 and are disrupted by Alzheimer-related PS1 mutations. Cell. 2010;141(7):1146-58. Epub 2010/06/15. doi: S0092-8674(10)00544-1 [pii]
10.1016/j.cell.2010.05.008. PubMed PMID: 20541250.
61. Wong BX, Tsatsanis A, Lim LQ, Adlard PA, Bush AI, Duce JA. beta-Amyloid precursor protein does not possess ferroxidase activity but does stabilize the cell surface ferrous iron exporter ferroportin. PLoS One. 2014;9(12):e114174. doi: 10.1371/journal.pone.0114174. PubMed PMID: 25464026; PubMed Central PMCID: PMC4252103.
62. Duce JA, Tsatsanis A, Cater MA, James SA, Robb E, Wikhe K, et al. Iron-export ferroxidase activity of beta-amyloid precursor protein is inhibited by zinc in Alzheimer's disease. Cell. 2010;142(6):857-67. doi: 10.1016/j.cell.2010.08.014. PubMed PMID: 20817278; PubMed Central PMCID: PMC2943017.
63. Buckland PR. Allele-specific gene expression differences in humans. Hum Mol Genet. 2004;13 Spec No 2:R255-60. Epub 2004/09/11. doi: 10.1093/hmg/ddh227. PubMed PMID: 15358732.
64. de la Chapelle A. Genetic predisposition to human disease: allele-specific expression and low-penetrance regulatory loci. Oncogene. 2009;28(38):3345-8. Epub 2009/07/15. doi: 10.1038/onc.2009.194. PubMed PMID: 19597467; PubMed Central PMCID: PMCPMC4348697.
65. Huang WC, Ferris E, Cheng T, Horndli CS, Gleason K, Tamminga C, et al. Diverse Non-genetic, Allele-Specific Expression Effects Shape Genetic Architecture at the Cellular Level in the Mammalian Brain. Neuron. 2017;93(5):1094-109 e7. Epub 2017/02/28. doi: 10.1016/j.neuron.2017.01.033. PubMed PMID: 28238550; PubMed Central PMCID: PMCPMC5774018.
66. Deng Q, Ramskold D, Reinius B, Sandberg R. Single-cell RNA-seq reveals dynamic, random monoallelic gene expression in mammalian cells. Science.

2014;343(6167):193-6. Epub 2014/01/11. doi: 10.1126/science.1245316. PubMed PMID: 24408435.
67. Newman M, Nornes S, Martins RN, Lardelli MT. Robust homeostasis of Presenilin1 protein levels by transcript regulation. Neuroscience letters. 2012;519(1):14-9. doi: 10.1016/j.neulet.2012.04.064. PubMed PMID: 22580062.
68. Jin H, Sanjo N, Uchihara T, Watabe K, St George-Hyslop P, Fraser PE, et al. Presenilin-1 holoprotein is an interacting partner of sarco endoplasmic reticulum calcium-ATPase and confers resistance to endoplasmic reticulum stress. Journal of Alzheimer's disease : JAD. 2010;20(1):261-73. Epub 2010/02/19. doi: 10.3233/JAD-2010-1360. PubMed PMID: 20164584.
69. Arensdorf AM, Diedrichs D, Rutkowski DT. Regulation of the transcriptome by ER stress: non-canonical mechanisms and physiological consequences. Front Genet. 2013;4:256. Epub 2013/12/19. doi: 10.3389/fgene.2013.00256. PubMed PMID: 24348511; PubMed Central PMCID: PMCPMC3844873.
70. Goetz AE, Wilkinson M. Stress and the nonsense-mediated RNA decay pathway. Cell Mol Life Sci. 2017;74(19):3509-31. Epub 2017/05/16. doi: 10.1007/s00018-017-2537-6. PubMed PMID: 28503708; PubMed Central PMCID: PMCPMC5683946.
71. Takami K, Terai K, Matsuo A, Walker DG, McGeer PL. Expression of presenilin-1 and -2 mRNAs in rat and Alzheimer's disease brains. Brain Res. 1997;748(1-2):122-30. Epub 1997/02/14. PubMed PMID: 9067452.
72. Isoe-Wada K, Urakami K, Wakutani Y, Adachi Y, Arai H, Sasaki H, et al. Alteration in brain presenilin-1 mRNA expression in sporadic Alzheimer's disease. Eur J Neurol. 1999;6(2):163-7.
73. Ikeda K, Urakami K, Arai H, Wada K, Wakutani Y, Ji Y, et al. The expression of presenilin 1 mRNA in skin fibroblasts and brains from sporadic Alzheimer's disease. Dement Geriatr Cogn Disord. 2000;11(5):245-50. Epub 2000/08/15. doi: 10.1159/000017246. PubMed PMID: 10940675.
74. Borghi R, Piccini A, Barini E, Cirmena G, Guglielmotto M, Tamagno E, et al. Upregulation of presenilin 1 in brains of sporadic, late-onset Alzheimer's disease. Journal of Alzheimer's disease : JAD. 2010;22(3):771-5. Epub 2010/09/18. doi: 10.3233/JAD-2010-100729. PubMed PMID: 20847436.
75. Farnsworth B, Peuckert C, Zimmermann B, Jazin E, Kettunen P, Emilsson LS. Gene Expression of Quaking in Sporadic Alzheimer's Disease Patients is Both Upregulated and Related to Expression Levels of Genes Involved in Amyloid Plaque and Neurofibrillary Tangle Formation. Journal of Alzheimer's disease : JAD. 2016;53(1):209-19. Epub 2016/05/11. doi: 10.3233/JAD-160160. PubMed PMID: 27163826; PubMed Central PMCID: PMCPMC4942724.
76. Johnston JA, Froelich S, Lannfelt L, Cowburn RF. Quantification of presenilin-1 mRNA in Alzheimer's disease brains. FEBS Lett. 1996;394(3):279-84. Epub 1996/10/07. PubMed PMID: 8830658.
77. Delabio R, Rasmussen L, Mizumoto I, Viani GA, Chen E, Villares J, et al. PSEN1 and PSEN2 gene expression in Alzheimer's disease brain: a new approach. Journal of Alzheimer's disease : JAD. 2014;42(3):757-60. Epub 2014/06/15. doi: 10.3233/JAD-140033. PubMed PMID: 24927704.
78. Fazekas de St G. The evaluation of limiting dilution assays. J Immunol Methods. 1982;49(2):R11-23. PubMed PMID: 7040548.

Figure Legends

Figure 1. Allele-specific *psen1* transcript expression in 6-month-old and 24-month-old zebrafish brains under normoxia and hypoxia. Each data point on the graph indicates *psen1* transcript copy number in 25ng of cDNA generated from a single zebrafish brain RNA sample. The age and genotype of each sample is indicated at the top of the graph. Grey bands indicate the hypoxia-treated samples. Wild type (+/+), *psen1*$^{K97fs/+}$ (K97fs/+) heterozygous mutant and *psen1*$^{Q96\_K97del/+}$ (Q96_K97del/+) heterozygous mutant. (*) indicates p-value < 0.05 by t-test: Two-Sample Assuming Unequal Variances. Raw dqPCR data, p-values and fold change comparisons indicated in the text are given in Supp. Data 1. **A.** Allele-specific expression of either wild type *psen1* (+, black circles) or mutant *psen1* (K97fs, red squares) (all females). **B.** Allele-specific expression of wild type *psen1* (+, black circles) and mutant *psen1* (Q96_K97del, red squares) (all males).

Figure 2. Hypoxia response gene expression in 6-month-old, 24-month-old and 42-month-old zebrafish brains under normoxia and hypoxia. Each data point on the graph indicates the relative transcript level for *cd44* (●), *edn1* (■), *igfbp3* (▲), *mmp2* (▼) and *pdk1* (◆) in 50ng of cDNA generated from a single zebrafish brain RNA sample (closed symbols: females, open symbols: males). Copy numbers for each transcript in each sample were scaled to the normalized means of the transcript copy numbers in the wild type 6 month normoxia samples. The age and genotype of each sample is indicated at the top of the graph. Grey bands indicate the hypoxia-treated samples. Wild type (+/+), *psen1*$^{K97fs/+}$ (K97fs/+) heterozygous mutant and *psen1*$^{Q96\_K97del/+}$ (Q96_K97del/+) heterozygous mutant. p-value < 0.05 for differentially expressed (DE) genes determined by t-test: Two-Sample Assuming Unequal Variances. Solid lines between bi-directional arrows indicate comparisons

for t-tests. The significantly differentially expressed genes are indicated below the bidirectional arrow. HRGs are HIF-1-responsive genes. The colour of the solid lines indicates the direction of differential expression; green indicates increase expression and red indicates decreased expression. Green and red arrows indicate the direction of *pdk1* expression change under hypoxia (arrow ends connect *pdk1* expression means). The raw dqPCR data, p-values and fold change comparisons indicated in text are given in Supp. Data 3. **A.** Hypoxia response gene expression in K97fs/+ and +/+ siblings (6 months and 24 months). **B.** Hypoxia response gene expression in Q96_K97del/+ and +/+ siblings (6, 24 and 42 months).

Figure 3. Lactate in 7-month-old and 31-month-old zebrafish brains under normoxia and hypoxia. Each data point on the graph indicates lactate content in a single whole zebrafish brain. All zebrafish were female. The age and genotype of each sample is indicated at the top of the graph. Grey bands indicate the hypoxia-treated samples. Wild type (+/+) and *psen1*$^{Q96\_K97del/+}$ (Q96_K97del/+) heterozygous mutant. P-values are calculated using t-test: Two-Sample Assuming Unequal Variances. Raw lactate assay data is given in Supp. Data 4. Lactate concentration is expressed as nmol per mg of whole brain from Q96_K97del/+ zebrafish and their +/+ siblings.

Figure 4. Hif1ab protein levels in 6-month-old and 24-month-old zebrafish brains under normoxia and hypoxia. Each data point on the graph indicates the Hif1ab protein level in protein extracted from a single zebrafish brain (closed circles: females, open cirlces: males). The age and genotype of each sample is indicated at the top of the graph. Grey bands indicate the hypoxia-treated samples. Wild type (+/+),

psen1$^{K97fs/+}$ (K97fs/+) heterozygous mutant and *psen1*$^{Q96\_K97del/+}$ (Q96_K97del/+) heterozygous mutant. (*) indicates p-value < 0.05 by t-test: Two-Sample Assuming Unequal Variances performed on Ln transformed data. Raw densitometry data and p-values are given in Supp. Data 2 and western blot images are shown in Supp. Figure 1. **A.** Hif1ab protein level in K97fs/+ and +/+ siblings. **B.** Hif1ab protein level in Q96_K97del/+ and +/+ siblings.

Figure 5. *PSEN1* and *PSEN2* transcript expression in the middle temporal gyrus region of brains of *PSEN1* mutation carriers and age-matched controls. Age-matched control (control, with corresponding carrier sample in parentheses), *PSEN1*$^{L271V/+}$ heterozygous mutation carrier (L271V/+), *PSEN1*$^{L219P/+}$ heterozygous mutation carrier (L219P /+) and *PSEN1*$^{G206V/+}$ heterozygous mutation carrier (G206V/+). Raw dqPCR data is given in Supp. Data 1. **A.** Expression of wild type (*PSEN1*$^{+}$) and L271V mutant (*PSEN1*^{L271V}) alleles in control and L271V/+ samples. **B.** Expression of either wild type (*PSEN1*$^{+}$) and L219P mutant (*PSEN1*^{L219P}) alleles in control and L219P/+ samples. **C.** Expression of either wild type (*PSEN1*$^{+}$) and G206V (*PSEN1*^{G206V}) alleles in control and G206V/+ samples. **D.** Expression of wild type *PSEN2* in all samples.

Supplementary Information

Supplementary Data 1. Presenilin allele-specific dqPCR data.

Supplementary Data 2. Hif1ab western blot densitometry data.

Supplementary Data 3. Hypoxia Response Genes dqPCR data

Supplementary Data 4. Lactate colorimetric assay data.

Supplementary Figure 1. Hif1ab western blot images.

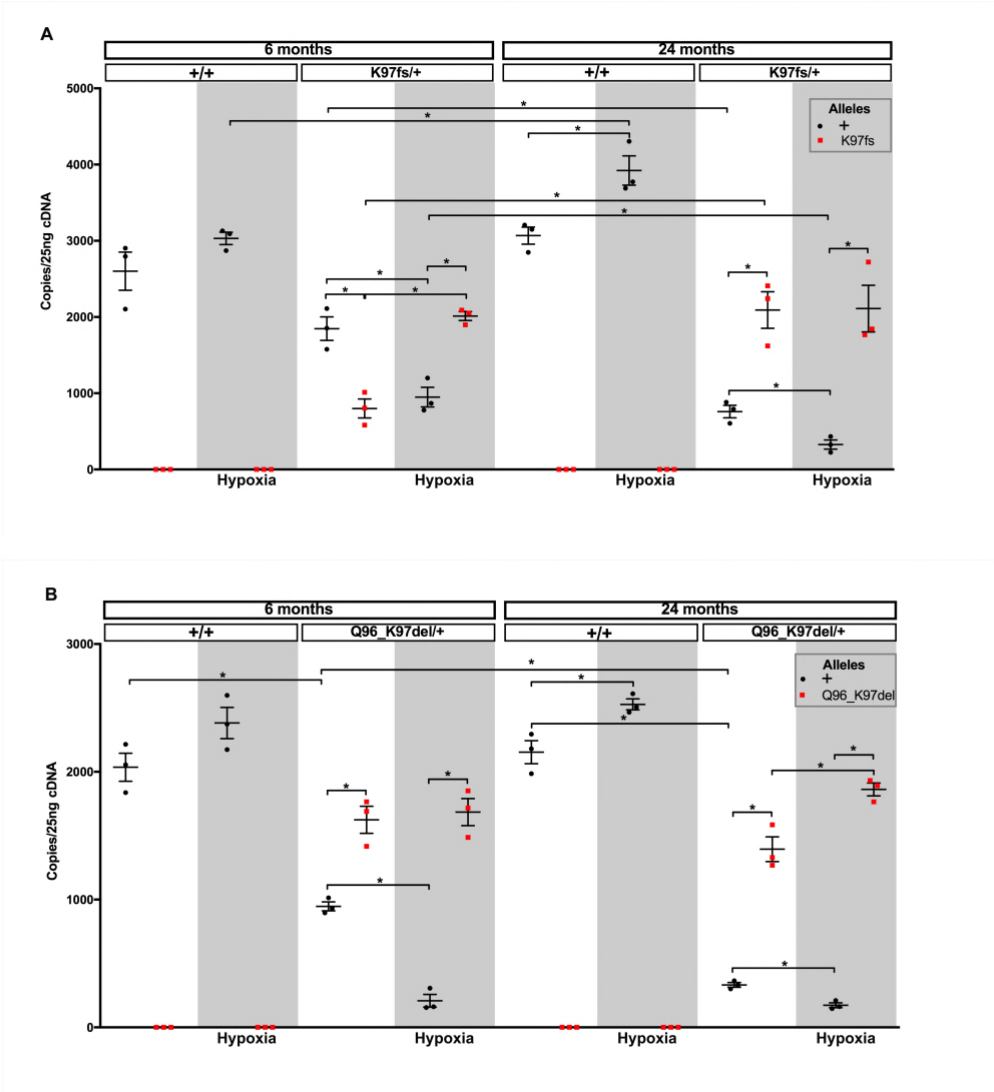

Figure 1.

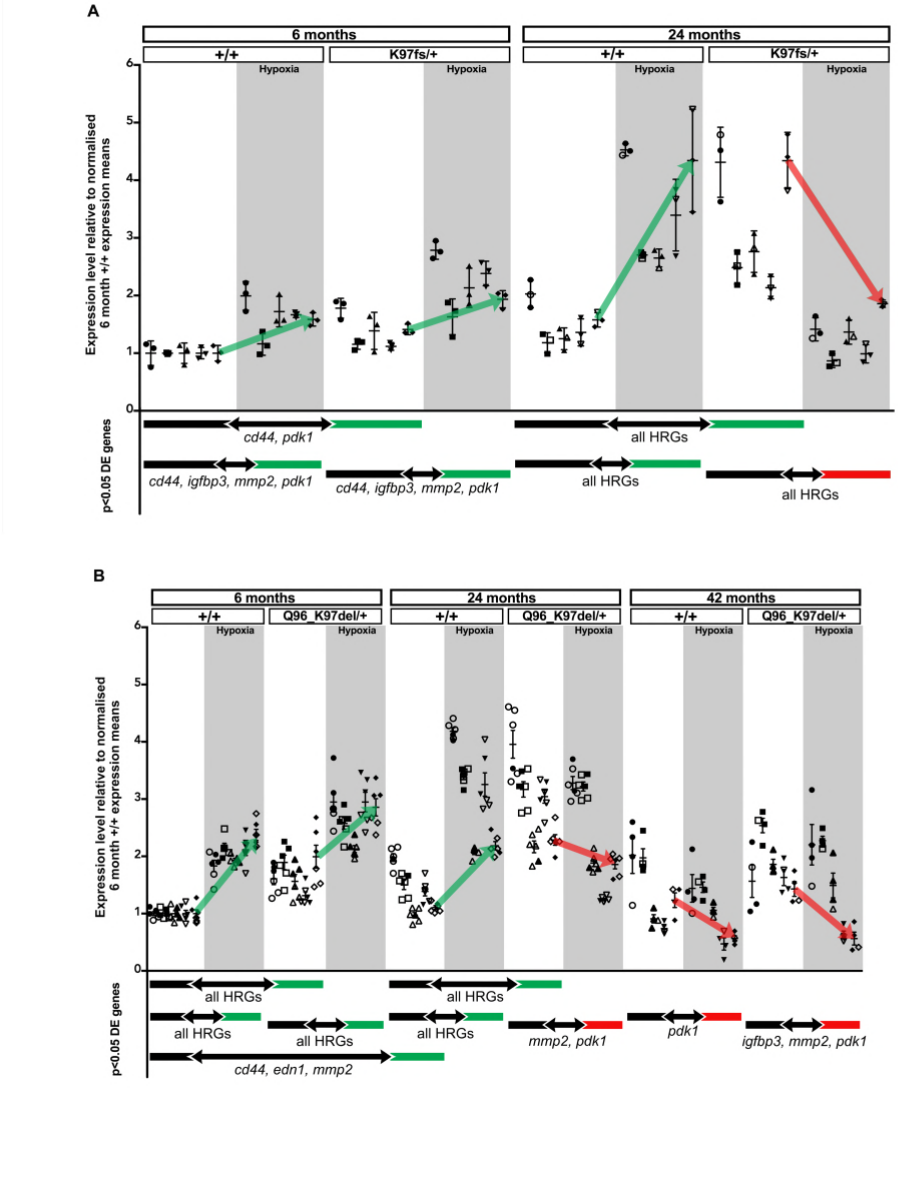

Figure 2.

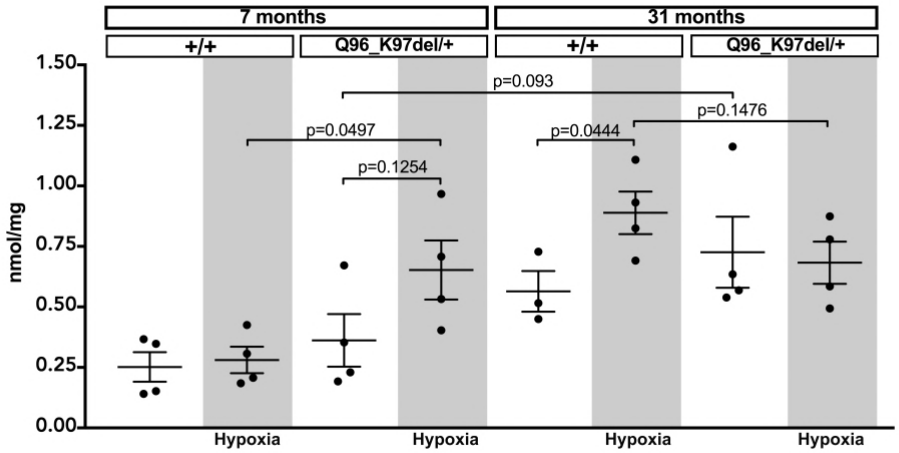

Figure 3.

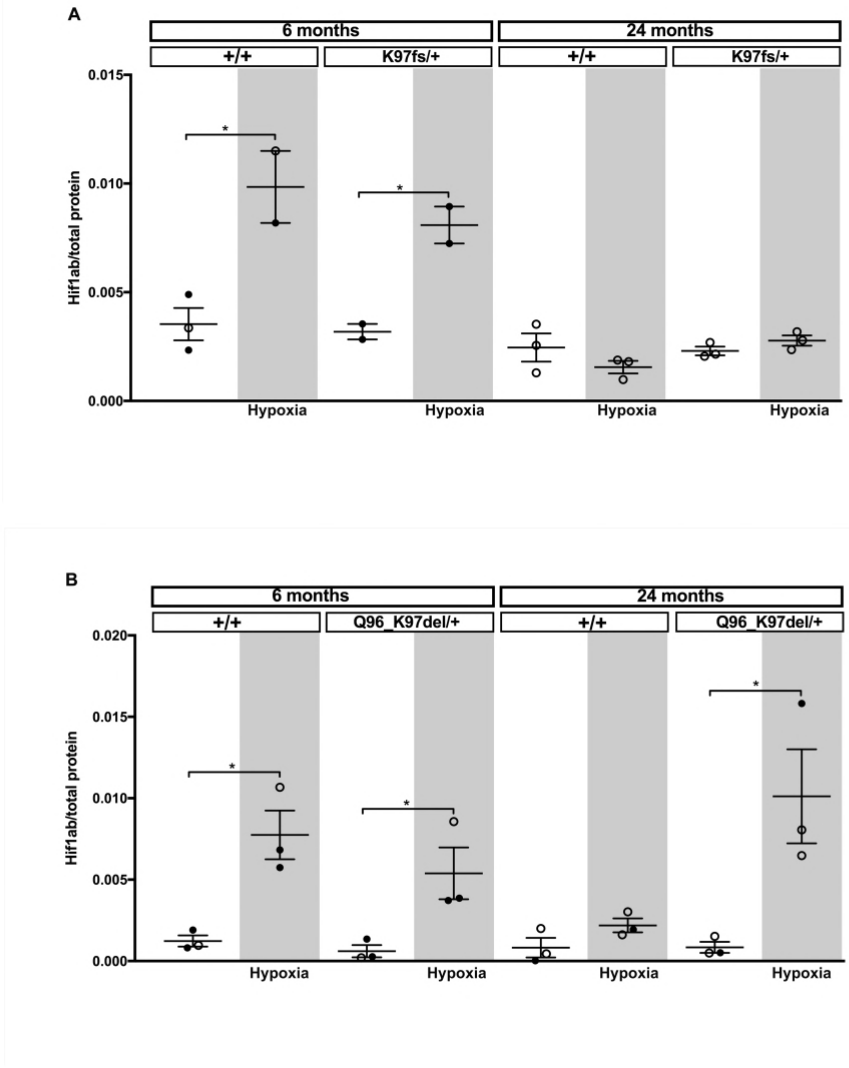

Figure 4.

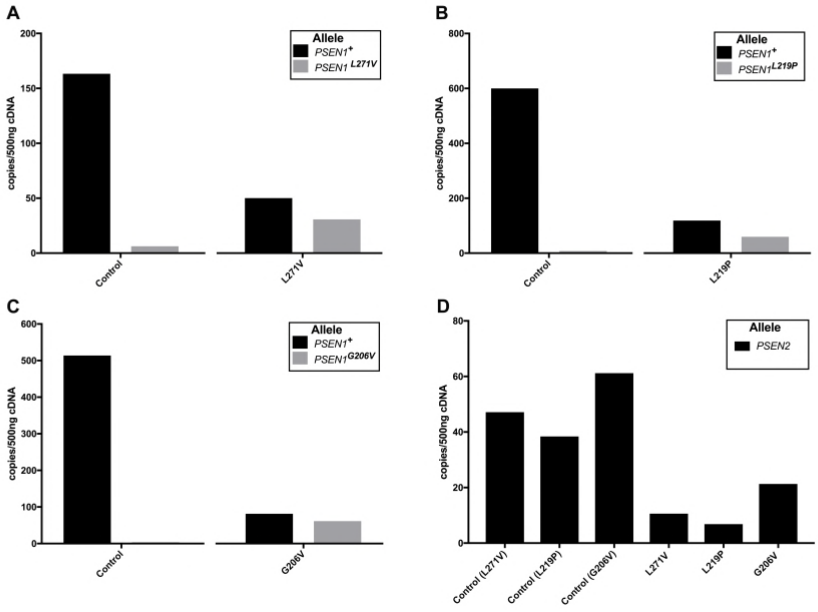

Figure 5.

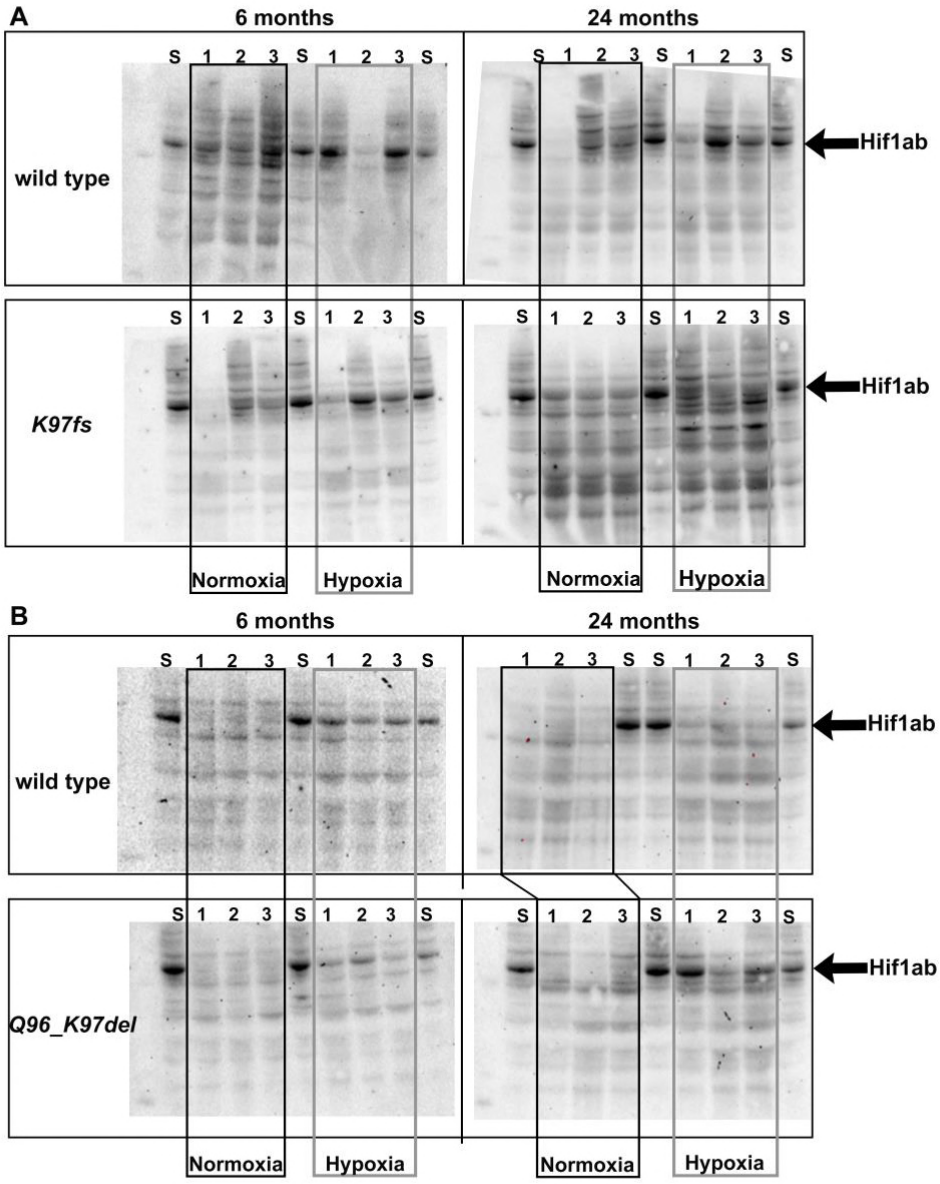

Supplementary Figure.